

## Mixed Azide and 5-(Pyrimidyl)tetrazole Bridged Co(II)/Mn(II) Polymers: Synthesis, Crystal Structures, Ferroelectric and Magnetic Behavior

Oindrila Sengupta and Partha Sarathi Mukherjee\*

Department of Inorganic and Physical Chemistry, Indian Institute of Science, Bangalore-560012, India

Received June 17, 2010

The reaction of pyrimidine-2-carbonitrile,  $\text{NaN}_3$  in the presence of  $\text{Co}(\text{NO}_3)_2 \cdot 6\text{H}_2\text{O}$  or  $\text{MnCl}_2 \cdot 4\text{H}_2\text{O}$  leads to the formation of complexes  $[\text{Co}(\text{pmtz})(\mu_{1,3}\text{-N}_3)(\text{H}_2\text{O})]_n$  (**1**) and  $[\text{Mn}(\text{pmtz})(\mu_{1,3}\text{-N}_3)(\text{H}_2\text{O})]_n$  (**2**) respectively, under hydrothermal condition [pmtz = 5-(pyrimidyl)tetrazolate]. These two complexes have been fully characterized by single crystal X-ray diffraction. Complex **1** crystallizes in a non-centrosymmetric space group  $Aba2$  in the orthorhombic system and is found to exhibit ferroelectric behavior, whereas complex **2** crystallizes in the  $P2_1/c$  space group in the monoclinic system. Variable temperature magnetic characterizations in the temperature range of 2–300 K indicate that complex **1** is a canted antiferromagnet (weak ferromagnet) with  $T_c = 15.9$  K. Complex **1** represents a unique example of a multiferroic coordination polymer containing tetrazole as a co-ligand. Complex **2** is a one-dimensional chain of Mn(II) bridged by a well-known antiferromagnetic coupler end-to-end azido ligand. In contrast to the role played by the end-to-end azido pathway in most of the transition metal complexes, complex **2** showed unusual ferromagnetic behavior below 40 K because of spin canting.

### Introduction

The chemistry of coordination polymers has become a promising field of research for the past few decades because of their immense applications in catalysis,<sup>1</sup> gas storage,<sup>2</sup>

magnetic materials,<sup>3</sup> optoelectronics<sup>4</sup> as well as in electrical conductivity.<sup>5</sup> The proper choice of metal ions and bridging ligands leads to different architectures whereas other parameters like metal ligand ratio, solvent, and temperature can also influence the outcome.<sup>6</sup> Magnetic coordination polymers are generally prepared via a building block approach using paramagnetic metal ions as nodes connected by bridging ligands that can efficiently transmit the magnetic exchange interactions between the metal centers to develop interesting magnetic properties.<sup>7–9</sup> In this respect several bridging ligands like cyanide, oxo, carboxylate, azide dominate in the literature because they are known to be good mediators for transmitting magnetic coupling between paramagnetic metal centers because of their short lengths. But still

\*To whom correspondence should be addressed. E-mail: psm@ipc.iisc.ernet.in. Fax: 91-80-23601552. Phone: 91-80-22933352.

(1) (a) Seo, S. J.; Whang, W.; Lee, H.; Jun, S. I.; Oh, J.; Jeon, Y. J.; Kim, K. *Nature* **2000**, *404*, 982. (b) Lee, J. Y.; Farha, O. K.; Roberts, J.; Scheidt, K. A.; Nguyen, S. T. *Chem. Soc. Rev.* **2009**, *38*, 1450. (c) Bannerjee, M.; Das, S.; Yoon, M.; Choi, J. H.; Hyun, M. H.; Park, S. M.; Seo, G.; Kim, K. *J. Am. Chem. Soc.* **2009**, *131*, 7524. (d) Kim, K. *Nat. Chem.* **2009**, *1*, 603. (e) Toh, N. L.; Nagarathinam, M.; Vittal, J. J. *Angew. Chem., Int. Ed.* **2005**, *44*, 2237.

(2) (a) Han, S. S.; Mendoza-Cortés, J. L.; Goddard, W. A., III *Chem. Soc. Rev.* **2009**, *38*, 1460. (b) Yaghi, O. M.; O'Keeffe, M.; Ockwig, N. W.; Chae, H. K.; Eddaoudi, M.; Kim, J. *Nature* **2003**, *423*, 705. (c) Férey, G. *Chem. Soc. Rev.* **2008**, *37*, 191. (d) Liu, X.; Park, M.; Hong, S.; Oh, M.; Yoon, J. Y.; Chong, J. S.; Lah, M. S. *Inorg. Chem.* **2009**, *48*, 11507. (e) Park, J.; Hong, S.; Moon, D.; Park, M.; Lee, K.; Kang, S.; Zou, Y.; John, R. P.; Kim, G. H.; Lah, M. S. *Inorg. Chem.* **2007**, *46*, 10208. (f) Hasegawa, S.; Horike, S.; Matsuda, R.; Furukawa, S.; Mochikuzi, K.; Kinoshita, Y.; Kitagawa, S. *J. Am. Chem. Soc.* **2007**, *129*, 2607. (g) Chatterjee, B.; Noveron, J. C.; Resendiz, M. J. E.; Liu, J.; Yamamoto, T.; Parker, D.; Cinke, M.; Arif, A. M.; Stang, P. J. *J. Am. Chem. Soc.* **2004**, *126*, 10645.

(3) (a) Kurmoo, M. *Chem. Soc. Rev.* **2009**, *38*, 1353. (b) Gatteschi, D.; Sessoli, R.; Cornia, A. *Chem. Commun.* **2000**, 725. (c) Rettig, S. J.; Sánchez, V.; Storr, A.; Thompson, R. C.; Trotter, J. *J. Chem. Soc., Dalton Trans.* **2000**, 3931.

(4) (a) Allendorf, M. D.; Bauer, C. A.; Bhakta, R. K.; Houk, R. J. *J. Am. Chem. Soc.* **2009**, *38*, 1330. (b) Chen, W.; Yuan, H. M.; Wang, J. Y.; Liu, Z. Y.; Xu, J. J.; Yang, M.; Chen, J. S. *J. Am. Chem. Soc.* **2003**, *125*, 9266. (c) Cariati, E.; Pizzotti, M.; Roberto, D.; Tessore, F.; Ugo, R. *Coord. Chem. Rev.* **2006**, *250*, 1210.

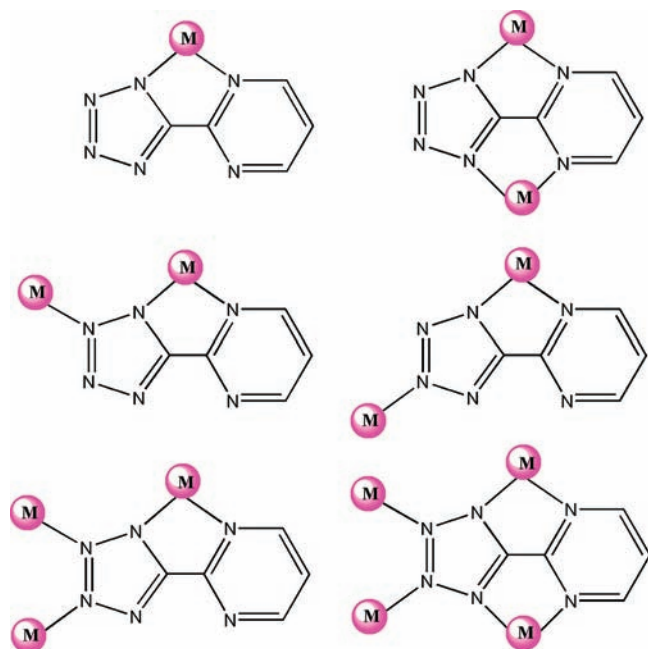
(5) Fang, Q. R.; Zhu, G. S.; Xue, M.; Zhang, Q. L.; Sun, J. Y.; Guo, X. D.; Qiu, S. L.; Xu, S. T.; Wang, P.; Wang, D. J.; Wei, Y. *Chem.—Eur. J.* **2006**, *12*, 3754.

(6) (a) Tong, M. L.; Hu, S.; Wang, J.; Kitagawa, S.; Ng, S. W. *Cryst. Growth Des.* **2005**, *5*, 837. (b) Naiya, S.; Biswas, C.; Drew, M. G. B.; Gómez-García, C. J.; Clemente-Juan, J. M.; Ghosh, A. *Inorg. Chem.* **2010**, *49*, 6616.

(7) (a) Jia, H.-P.; Zhan-Feng Ju, W. L.; Zhang, J. *Chem. Commun.* **2008**, 371. (b) Palli, A. V.; Reu, O. S.; Ostrovsky, S. M.; Klokishner, S. I.; Tsukerblat, B. S.; Sun, Z.-M.; Mao, J.-G.; Prosvirin, A. V.; Zhao, H.-H.; Dunbar, K. R. *J. Am. Chem. Soc.* **2008**, *130*, 14729. (c) Li, J.-R.; Yu, Q.; Tao, Y.; Bu, X.-H.; Ribas, J.; Batten, S. R. *Chem. Commun.* **2007**, 2290. (d) Cao, D.-K.; Li, Y.-Z.; Zheng, L. M. *Inorg. Chem.* **2007**, *46*, 7571.

(8) (a) Sourlas, N. *Nature* **1989**, *339*, 693. (b) Taniguchi, T.; Yamanaka, K.; Sumioka, H.; Yamazaki, T.; Tabata, Y.; Kawarazaki, S. *Phys. Rev. Lett.* **2004**, *93*, 246605. (c) Liu, X.-T.; Wang, X.-Y.; Zhang, W.-X.; Cui, P.; Gao, S. *Adv. Mater.* **2006**, *18*, 2852.

(9) (a) Figuerola, A.; Tangoulis, V.; Ribas, J.; Hartl, H.; Brudgam, I.; Maestro, M.; Diaz, C. *Inorg. Chem.* **2007**, *46*, 11017. (b) Prinz, M.; Kuepper, K.; Taubitz, C.; Raekers, M.; Khanra, S.; Biswas, B.; Weyhermüller, T.; Uhlarz, M.; Wosnitzer, J.; Schnack, J.; Postnikov, A. V.; Schröder, C.; George, S. J.; Neumann, M.; Chaudhuri, P. *Inorg. Chem.* **2010**, *49*, 2093.

**Scheme 1.** Some Possible Coordination Modes of 5-(Pyrimidyl)tetrazolate

there is a surge in the search for a new bridging ligand that can lead to new magnetic materials. In this regard, nitrogen containing heterocyclic ligands like pyrazole, imidazole, and tetrazole are now receiving considerable attention.<sup>10</sup> Tetrazole based ligands are now in prime focus because of their rich coordination chemistry that leads to great variety of interesting structures.<sup>11–13</sup> 5-(Pyrimidyl)tetrazole ligand is found to be an excellent and versatile building block having multicoordination sites (Scheme 1).<sup>14</sup> The ligand possesses six basic nitrogen atoms having both pyrimidine and tetrazole functionality. In the past few years several works have been carried out with substituted tetrazoles.<sup>15–18</sup> Though a few metal complexes of (5-pyrimidyl)tetrazole are reported, very little is known where a secondary bridging ligand like azide has been incorporated to increase the dimensionality.<sup>14</sup> As far as our knowledge is concerned, only one Cd(II) complex is reported having both the tetrazole and the azide

until today.<sup>19</sup> As it has been proved that azide is an excellent candidate for the propagation of magnetic interaction between paramagnetic metal centers with different magnetic properties by virtue of its several bridging modes,<sup>20,21</sup> we thought to include its functionality in the metal tetrazole systems and study their properties. It is well established that among various bridging modes,  $\mu_{1,1}$ -(end-on, EO) favors ferromagnetic coupling whereas  $\mu_{1,3}$ -(end-to-end, EE) prefers antiferromagnetic interaction.<sup>21</sup> An example of end-to-end mode for an azide group with ferromagnetic coupling is still rare although such systems are favored according to theoretical calculations.<sup>22–24</sup>

On the other hand ferroelectric materials are of great interests because of their promising applications in electric devices, such as dynamic random access memories, binary data storage media, and also in telecommunication systems.<sup>25,26</sup> The quest for multiferroic materials, where both ferroelectricity as well as magnetism coexist, is of great technological and fundamental importance.<sup>27</sup> Multiferroics are very rare since ferroelectricity and magnetism interact weakly with each other when they coexist.<sup>28</sup> The present paper reports the synthesis, crystal structures, and variable temperature magnetic characterizations of two coordination polymers  $[\text{Co}(\text{pmtz})(\mu_{1,3}\text{-N}_3)(\text{H}_2\text{O})]_n$  (**1**) and  $[\text{Mn}(\text{pmtz})(\mu_{1,3}\text{-N}_3)(\text{H}_2\text{O})]_n$  (**2**) using pmtz in combination with a secondary bridging azide ligand. Though a few examples of tetrazole based ferroelectric materials are reported recently,<sup>25b</sup>

(19) Rodríguez-Diéguez, A.; Salinas-Castillo, A.; Galli, S.; Masciocchi, N.; Gutiérrez-Zorrilla, J. M.; Vitoria, P.; Colacio, E. *Dalton Trans.* **2007**, 1821.

(20) Ribas, J.; Escuer, A.; Monfort, M.; Vicente, R.; Cortés, R.; Lezama, L.; Rojo, T. *Coord. Chem. Rev.* **1999**, *193*, 1027.

(21) (a) Kahn, O.; Sikorav, S.; Gouteron, J.; Jeannin, S.; Jeannin, Y. *Inorg. Chem.* **1983**, *22*, 2877. (b) Sikorav, S.; Bkouche-Waksman, I.; Kahn, O. *Inorg. Chem.* **1984**, *23*, 490. (c) Wang, Y.-Q.; Jia, Q.-X.; Wang, K.; Cheng, A.-L.; Gao, E.-Q. *Inorg. Chem.* **2010**, *49*, 1551. (d) Charlot, M. F.; Kahn, O.; Chaillet, M.; Larrieu, C. *J. Am. Chem. Soc.* **1986**, *108*, 2574. (e) Cortés, R.; Pizarro, J. L.; Lezama, L.; Arriortua, M. I.; Rojo, T. *Inorg. Chem.* **1994**, *33*, 2697. (f) Ribas, J.; Monfort, M.; Diaz, C.; Bastos, C.; Solans, X. *Inorg. Chem.* **1994**, *33*, 484. (g) Ruiz, E.; Cano, J.; Alvarez, S.; Alemany, P. *J. Am. Chem. Soc.* **1998**, *120*, 11122.

(22) (a) Ribas, J.; Monfort, M.; Ghosh, B. K.; Cortés, R.; Solans, X.; Font-Bardía, M. *Inorg. Chem.* **1996**, *35*, 864. (b) Escuer, A.; Vicente, R.; Ribas, J.; El Fallah, M. S.; Solans, X.; Font-Bardía, M. *Inorg. Chem.* **1994**, *33*, 1842. (c) Vicente, R.; Escuer, A.; Ribas, J.; El Fallah, M. S.; Solans, X.; Font-Bardía, M. *Inorg. Chem.* **1995**, *34*, 1278.

(23) (a) Hong, C. S.; Do, Y. *Angew. Chem., Int. Ed.* **1999**, *38*, 193. (b) Maji, T. K.; Mukherjee, P. S.; Mostafa, G.; Mallah, T.; Cano-Boquera, J.; Chaudhuri, N. R. *Chem. Commun.* **2001**, 1012. (c) Mukherjee, P. S.; Dalai, S.; Zangrando, E.; Lloret, F.; Chaudhuri, N. R. *Chem. Commun.* **2001**, 1444. (d) Escuer, A.; Harding, C. J.; Dussart, Y.; Nelson, J.; McKee, V.; Vicente, R. *J. Chem. Soc., Dalton Trans.* **1999**, 223. (e) Shen, Z.; Zuo, J.-L.; Gao, S.; Song, Y.; Che, C.-M.; Fun, H.-K.; You, X.-Z. *Angew. Chem., Int. Ed.* **2000**, *39*, 3633. (f) de-Biani, F. F.; Ruiz, E.; Cano, J.; Novoa, J. J.; Alvarez, S. *Inorg. Chem.* **2000**, *39*, 3221. (g) Li, L.; Liao, D.; Jiang, Z.; Yan, S. *Inorg. Chem.* **2002**, *41*, 1019.

(24) Abu-Youssef, M. A. M.; Drillon, M.; Escuer, A.; Goher, M. A. S.; Mautner, F. A.; Vicente, R. *Inorg. Chem.* **2000**, *39*, 5022.

(25) (a) Zhang, W.; Ye, H.-Y.; Xiong, R.-G. *Coord. Chem. Rev.* **2009**, *253*, 2980. (b) Zhao, H.; Qu, Z.-R.; Ye, H.-Y.; Xiong, R.-G. *Chem. Soc. Rev.* **2008**, *37*, 84.

(26) (a) Jain, P.; Ramachandran, V.; Clark, R. J.; Zhou, H. D.; Toby, B. H.; Dalal, N. S.; Kroto, H. W.; Cheetham, A. K. *J. Am. Chem. Soc.* **2009**, *131*, 13625. (b) Ye, Q.; Fu, D.-W.; Tian, H.; Xiong, R.-G.; Chan, P. W. H.; Huang, S. D. *Inorg. Chem.* **2008**, *47*, 772. (c) Rogez, G.; Viart, N.; Drillon, M. *Angew. Chem., Int. Ed.* **2010**, *49*, 1921. (d) Ohkoshi, S.-I.; Tokoro, H.; Matsuda, T.; Takahashi, H.; Irie, H.; Hashimoto, K. *Angew. Chem., Int. Ed.* **2007**, *46*, 3228.

(27) (a) Rao, C. N. R.; Serrao, C. R. *J. Chem. Mater.* **2007**, *17*, 4931. (b) Jiang, Q. H.; Ma, J.; Lin, Y. H.; Nan, C. W.; Shi, Z.; Shen, Z. *J. Appl. Phys. Lett.* **2007**, *91*, 022914. (c) Khomskii, D. I. *J. Magn. Magn. Mater.* **2006**, *306*, 1.

(28) Azuma, M.; Takata, K.; Saito, T.; Ishiwata, S.; Shimakawa, Y.; Takano, M. *J. Am. Chem. Soc.* **2005**, *127*, 8889.

(10) (a) Huang, X.-C.; Lin, Y.-Y.; Zhang, J.-P.; Chen, X.-M. *Angew. Chem., Int. Ed.* **2006**, *45*, 1557. (b) Banerjee, R.; Phan, A.; Wang, B.; Knobler, C.; Furukawa, H.; O'Keeffe, M.; Yaghi, O. M. *Science* **2008**, *319*, 939. (c) Wang, B.; Côté, A. P.; Furukawa, H.; O'Keeffe, M.; Yaghi, O. M. *Nature* **2008**, *453*, 207.

(11) Rodríguez, A.; Kivekäs, R.; Colacio, E. *Chem. Commun.* **2005**, 5228.

(12) (a) Dinca, M.; Yu, A. F.; Long, J. R. *J. Am. Chem. Soc.* **2006**, *128*, 8904. (b) Dinca, M.; Long, J. R. *J. Am. Chem. Soc.* **2007**, *129*, 11172.

(13) (a) Xue, X.; Wang, X.; Wang, L.; Xiong, R.-G.; Abrahams, B. F.; You, X.; Xue, Z.; Che, C. *Inorg. Chem.* **2002**, *41*, 6544. (b) Tao, J.; Ma, Z. J.; Huang, R. B.; Zheng, J. S. *Inorg. Chem.* **2004**, *43*, 6133.

(14) (a) Rodríguez-Diéguez, A.; Palacios, M. A.; Sironi, A.; Colacio, E. *Dalton Trans.* **2008**, 2887. (b) Rodríguez-Diéguez, A.; Mota, A. J.; Seco, J. M.; Palacios, M. A.; Romerosa, A.; Colacio, E. *Dalton Trans.* **2009**, 9578. (c) Pachfule, P.; Das, R.; Poddar, P.; Banerjee, R. *Cryst. Growth Des.* **2010**, *10*, 1475. (d) Rodríguez-Diéguez, A.; Colacio, E. *Chem. Commun.* **2006**, 4140.

(15) Wu, T.; Yi, B.-H.; Li, D. *Inorg. Chem.* **2005**, *44*, 4130.

(16) Mautner, F. A.; Gspan, C.; Gatterer, K.; Goher, M. A. S.; Abu-Youssef, M. A. M.; Bucher, E.; Sitte, W. *Polyhedron* **2004**, *23*, 1217.

(17) (a) Lin, P.; Clegg, W.; Harrington, R. W.; Henderson, R. A. *Dalton Trans.* **2005**, 2388. (b) Mo, X.-J.; Gao, E.-Q.; He, Z.; Li, W.-J.; Yan, C.-H. *Inorg. Chem. Commun.* **2004**, *7*, 353.

(18) Abu-Youssef, M. A. M.; Mautner, F. A.; Massoud, A. A.; Öhrström, L. *Polyhedron* **2007**, *26*, 1531.

complex **1** represents a unique example of a tetrazole coordinated multiferroic system which shows ferroelectricity (down to 100 K) as well as a magnetic hysteresis loop (below 15 K). Complex **2** showed dominant antiferromagnetic behavior with an unusual ferromagnetic transition in the low temperature region because of spin canting.

### Experimental Section

**Materials.**  $\text{Co}(\text{NO}_3)_2 \cdot 6\text{H}_2\text{O}$ ,  $\text{MnCl}_2 \cdot 4\text{H}_2\text{O}$ , 2-cyanopyrimidine (Aldrich), and  $\text{NaN}_3$  are commercially available and were used without further purification. Elemental analyses of C, H, and N were performed using a Perkin-Elmer 240C elemental analyzer. IR spectra were recorded as KBr pellets using a Magna 750 FT-IR spectrophotometer. The variable temperature magnetic studies in the range of 2–300 K were carried out on crystalline samples using a Quantum Design MPMS-XL5 SQUID magnetometer. Powder X-ray diffraction (XRD) patterns of the complexes were measured in a D8 powder diffractometer. Ferroelectric measurement of complex **1** was performed on powder sample in the form of a pellet using a RT6000 ferroelectric tester.

**Synthesis of Complex  $[\text{Co}(\text{pmtz})(\mu_{1,3}\text{-N}_3)(\text{H}_2\text{O})]_n$  (**1**).** To a mixture of 2-cyanopyrimidine (53 mg, 0.5 mmol) and  $\text{NaN}_3$  (390 mg, 6 mmol) in water (10 mL)  $\text{Co}(\text{NO}_3)_2 \cdot 6\text{H}_2\text{O}$  was added (291 mg, 1 mmol). The resulting deep red solution was placed in a 23 mL Teflon-lined hydrothermal flask and was heated at 100 °C for 24 h. Red single crystals were obtained upon slow cooling of the solution to room temperature over a period of 6 h. Isolated yield: 75%. Anal. Calcd for **1**,  $\text{C}_5\text{H}_5\text{CoN}_9\text{O}$ : C, 22.55; N, 47.36; H, 1.87. Found: C, 22.73; N, 47.57; H, 1.99. IR( $\text{cm}^{-1}$ ): 2122, 1571(s).

**Synthesis of Complex  $[\text{Mn}(\text{pmtz})(\mu_{1,3}\text{-N}_3)(\text{H}_2\text{O})]_n$  (**2**).** Complex **2** was prepared in a similar way as employed in case of **1** by hydrothermal method using  $\text{MnCl}_2 \cdot 4\text{H}_2\text{O}$  (198 mg, 1 mmol) instead of  $\text{Co}(\text{NO}_3)_2 \cdot 6\text{H}_2\text{O}$ . Yellow crystals were obtained upon slow cooling of the reaction mixture to room temperature over a period of 10 h. Isolated yield: 71%. Anal. Calcd for **2**,  $\text{C}_5\text{H}_5\text{MnN}_9\text{O}$ : C, 22.90; N, 48.09; H, 1.90. Found: C, 23.17; N, 48.32; H, 2.09. IR( $\text{cm}^{-1}$ ): 2120, 1578(s).

**Caution!** Azido complexes of metal ions in the presence of organic ligands are potentially explosive. Only a small amount of material should be prepared, and it should be handled with care.

**X-ray Crystallographic Data Collection and Refinements.** Single crystal X-ray data of **1** and **2** were collected at 293 K, on a Bruker Apex-II CCD diffractometer equipped with graphite monochromated Mo–K $\alpha$  radiation ( $\lambda = 0.71073 \text{ \AA}$ ). The SMART program was used for data acquisition, while the SAINT program was used for data extraction.<sup>29</sup> The crystal structures were solved by direct methods using the SHELX-97<sup>30</sup> incorporated in WinGX.<sup>31</sup> Empirical absorption corrections were applied with SADABS.<sup>32</sup> All non-hydrogen atoms were refined anisotropically and were located on geometrically calculated positions. The hydrogen atoms were refined isotropically and assigned idealized positions and given thermal parameters equivalent to 1.2 times the thermal parameters of carbon atom to which they were attached. A summary of crystal data and structure refinements for complexes **1–2** are tabulated in Table 1.

**Table 1.** Crystallographic Data and Refinement Parameters for **1–2**

identification code	<b>1</b>	<b>2</b>
empirical formula	$\text{C}_5\text{H}_5\text{CoN}_9\text{O}$	$\text{C}_5\text{H}_5\text{MnN}_9\text{O}$
formula weight	264.09	262.12
temperature	293(2) K	293(2) K
wavelength	0.71073 Å	0.71073 Å
crystal system	orthorhombic	monoclinic
Space group	<i>Aba2</i>	<i>P2<sub>1</sub>/c</i>
<i>a</i> /Å	11.0858(7)	8.780(5)
<i>b</i> /Å	22.4539(14)	6.423(5)
<i>c</i> /Å	7.2261(5)	16.159(5)
$\alpha$ /deg	90	90
$\beta$ /deg	90	90.036(5)
$\gamma$ /deg	90	90
$V/\text{Å}^3$	1798.7(2)	911.3(9)
<i>Z</i>	8	4
density (calculated)	1.950 g/cm <sup>3</sup>	1.911 g/cm <sup>3</sup>
$\mu$	1.903 mm <sup>-1</sup>	1.444 mm <sup>-1</sup>
reflections collected	11649	13706
independent reflections	2731 [ <i>R</i> (int) = 0.0564]	2663 [ <i>R</i> (int) = 0.0433]
final <i>R</i> indices	<i>R</i> 1 = 0.0352	<i>R</i> 1 = 0.0433
[ <i>I</i> > 2 $\sigma$ ( <i>I</i> )]	<i>wR</i> 2 = 0.0698	<i>wR</i> 2 = 0.1010
<i>R</i> indices (all data)	<i>R</i> 1 = 0.0567	<i>R</i> 1 = 0.0507
	<i>wR</i> 2 = 0.0790	<i>wR</i> 2 = 0.1050

Selected bond parameters of the complexes are assembled in the Supporting Informations, Table S1.

### Results and Discussion

**Synthesis.** The ligand 5-(pyrimidyl)tetrazole was synthesized in situ by [2 + 3] cycloaddition of azide to 2-cyanopyrimidine. Such type of reaction leading to the formation of tetrazoles is well documented in the literature.<sup>11–18</sup> Metal ions Co(II) or Mn(II) upon reaction with 2-cyanopyrimidine in presence of excess azide formed the complexes **1** and **2**, respectively, under hydrothermal condition. Complex **1** was also obtained by treating  $\text{Co}(\text{NO}_3)_2 \cdot 6\text{H}_2\text{O}$  with a mixture of 1 equiv of Na-pmtz and excess  $\text{NaN}_3$  in water at room temperature. However, attempts to prepare these complexes using 1 equiv of azide at both room temperature and high temperature were unsuccessful. Hence, excess azide played an important role in driving the reaction toward the forward direction. The purity of both complexes was confirmed from their powder XRD diffraction patterns which matched well with the calculated patterns obtained from their single crystal X-ray structures (Figure 1). The peaks in the IR spectra of **1** and **2** at 1571, and 1578  $\text{cm}^{-1}$ (s) are due to the tetrazole moiety, and they also showed very intense peaks corresponding to azido at 2122 and 2120  $\text{cm}^{-1}$ , respectively.

### Structure Description

**Crystal Structure of 1.** Complex **1** crystallized in the orthorhombic space group *Aba2*, the asymmetric unit of which contains a [pmtz]<sup>-</sup> anion, one azide, and a water molecule. Only one type of Co(II) ion has been crystallographically identified. In this complex, Co(II) ion achieves a distorted octahedral geometry with  $\text{Co}(\text{N}_5)\text{O}$  core. The basic coordination environment around the Co(II) center with the atom numbering scheme is shown (see Supporting Information). The basic asymmetric unit of **1** consists of a pyrimidine N and a N from the tetrazole moiety of pmtz<sup>-</sup> ligand which were found to coordinate the metal center with bond lengths  $\text{Co}(1)\text{--N}(4) = 2.199(2) \text{ \AA}$

(29) SMART/SAINT; Bruker AXS, Inc.: Madison, WI, 2004.

(30) Sheldrick, G. M. *SHELX-97, Program for the Solution and Refinement of Crystal Structures*; University of Göttingen: Göttingen, Germany, 1998.

(31) Farrugia, L. J. *WinGX: An Integrated System of Windows Program for the Solution, Refinement and Analysis for Single Crystal X-ray Diffraction Data*, version 1.65.04; Department of Chemistry: University of Glasgow, 2003.

(32) Sheldrick, G. M. *SADABS, Bruker Nonius Area Detector Scaling and Absorption Correction*, version 2.05; University of Göttingen: Göttingen, Germany, 1999.



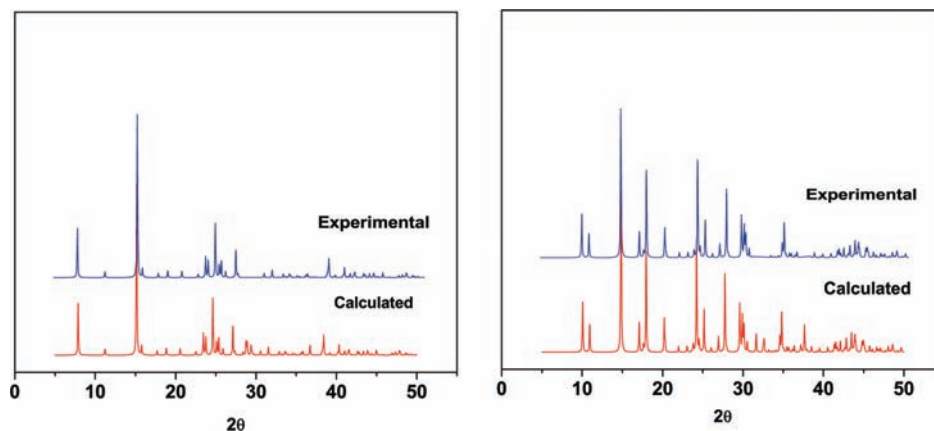


**Figure 1.** Calculated (red) and experimental (blue) powder XRD patterns of the complexes **1** (left) and **2** (right).

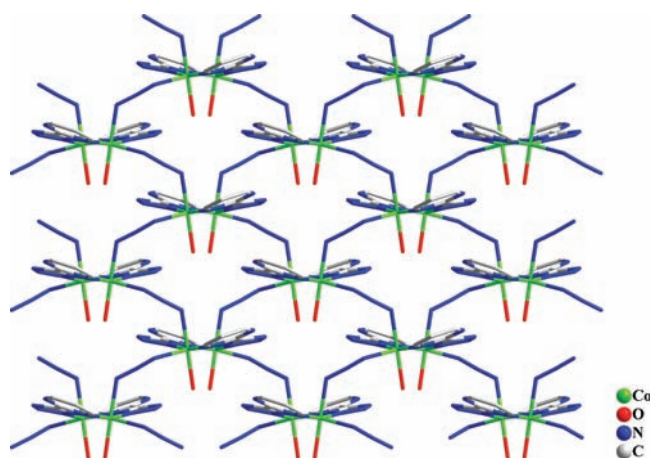


**Figure 2.** View of the 2D structure of complex **1** showing tetrahedral pockets formed by four neighboring dimeric fragments.

and  $\text{Co}(1)-\text{N}(6) = 2.108(2) \text{ \AA}$ , respectively. One  $\mu_{1,3}\text{-N}_3^-$  group was found to coordinate to  $\text{Co}(\text{II})$  ion having bond length  $\text{Co}(1)-\text{N}(1) = 2.144(3) \text{ \AA}$ . The fourth coordination site has been filled by a  $\text{H}_2\text{O}$  molecule with  $\text{Co}(1)-\text{O}(1) = 2.080(2) \text{ \AA}$ . The fifth and sixth coordination sites of each octahedral  $\text{Co}(\text{II})$  were satisfied by a second  $\mu_{1,3}\text{-N}_3^-$  and  $\text{pmtz}^-$  ligand that coordinate through their N atoms with bond lengths  $\text{Co}(1)-\text{N}(3)^a = 2.103(2) \text{ \AA}$  and  $\text{Co}(1)-\text{N}(7)^b = 2.120(2) \text{ \AA}$  from the neighboring unit. Coordination through the end-to-end azide ligand with the adjacent  $\text{Co}(\text{II})$  center forms a butterfly like dimeric unit (see Supporting Information), and each dimeric unit contains the pyrimidyl ring in a non planar bent form with a large  $\text{Co}-\text{N}_3-\text{Co}$  torsion angle of  $68.18(2)^\circ$ . Each dimeric fragment then connects to the nearest one through an end-to-end azide bridge and forms finally a 2D network (Figure 2). The sheet structure showed the formation of tetrahedral pockets by four neighboring dimeric units.

**Crystal Structure of 2.** Complex **2** crystallized in the monoclinic  $P2_1/c$  space group having one crystallographically distinguished octahedral  $\text{Mn}(\text{II})$  ion coordinated to one  $[\text{pmtz}]^-$  anion [ $\text{Mn}(1)-\text{N}(2) = 2.222(3) \text{ \AA}$ ], one  $\mu_{1,3}$ -azide [ $\text{Mn}(1)-\text{N}(7) = 2.184(3) \text{ \AA}$ ], and a water molecule [ $\text{Mn}(1)-\text{O}(1w) = 2.193(3) \text{ \AA}$ ] in the asymmetric unit (Supporting Information). The other three coordination sites have been fulfilled by one pyrimidine N of  $[\text{pmtz}]^-$  [ $\text{Mn}(1)-\text{N}(6)^c = 2.305(3) \text{ \AA}$ ], one N atom of

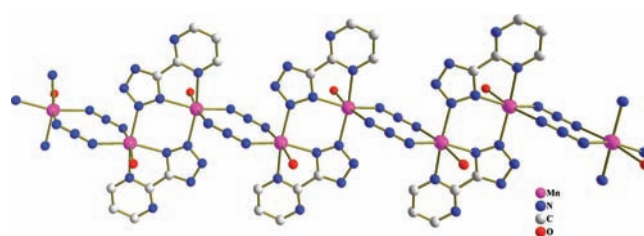


**Figure 3.** View of the 1D chain structure of **2** along the crystallographic  $a$  axis.

tetrazole moiety of the ligand [ $\text{Mn}(1)-\text{N}(1)^c = 2.249(3) \text{ \AA}$ ] and a N of  $\mu_{1,3}\text{-N}_3^-$  [ $\text{Mn}(1)-\text{N}(9)^d = 2.253(3) \text{ \AA}$ ] shared by the neighboring  $\text{Mn}(\text{II})$  center. Each  $\text{Mn}(\text{II})$  center in complex **2** is connected through double  $\mu_{1,3}\text{-N}_3^-$  bridges to form a dimeric unit (Supporting Information) with  $\text{Mn}-\text{N}_3-\text{Mn}$  torsion angle of  $29.45(5)^\circ$  having very large  $\text{Mn}(1)-\text{N}(7)-\text{N}(8)$  and  $\text{Mn}(1)-\text{N}(9)-\text{N}(8)$  angles of  $143.91(3)^\circ$  and  $115.8(2)^\circ$ , respectively. Finally these dimeric units extend through an end-to-end azide bridge to form an one-dimensional (1D) chain structure (Figure 3). Though both **1** and **2** contain the same asymmetric unit with an end-to-end azide bridge, complex **1** forms a two-dimensional (2D) network while complex **2** constitutes an 1D chain.

The packing diagram (Supporting Information) reveals that the 1D  $\text{Mn}(\text{II})$  chains in **2** extend to a 2D network through hydrogen bonding interactions between the nitrogen atom (N5) of the pyrimidine ring of 5-(pyrimidyl)-tetrazole ligand/ $\mu_{1,3}\text{-N}_3^-$  (N9) ligand with the coordinated water molecules. The hydrogen bonding parameters are tabulated in the Supporting Information, Table S2 (D = Donor, A = Acceptor).

**Magnetic Study of 1.** Magnetic susceptibility measurements were carried out on a crystalline sample of **1** with an applied magnetic field of 500 G in the temperature range 2–300 K using a quantum designed SQUID magnetometer. The magnetic properties of **1** in the form of  $\chi_M$  versus  $T$  and  $\chi_M T$  versus  $T$  per  $\text{Co}(\text{II})$  ion are presented in Figure 4. The  $\chi_M T$  value per  $\text{Co}(\text{II})$  unit at 300 K is  $2.35 \text{ cm}^3 \text{ mol}^{-1} \text{ K}$  which is higher than those expected for spin only value of  $1.87 \text{ cm}^3 \text{ mol}^{-1} \text{ K}$  for one uncoupled  $\text{Co}(\text{II})$  ion with  $S = 3/2$  spin. This higher value is presumably due to the presence of important orbital contributions which is common for  $\text{Co}(\text{II})$  high-spin octahedral complexes.  $\chi_M T$  gradually decreases upon cooling until it reaches a minimum of  $1.48 \text{ cm}^3 \text{ mol}^{-1} \text{ K}$  at 23 K, which

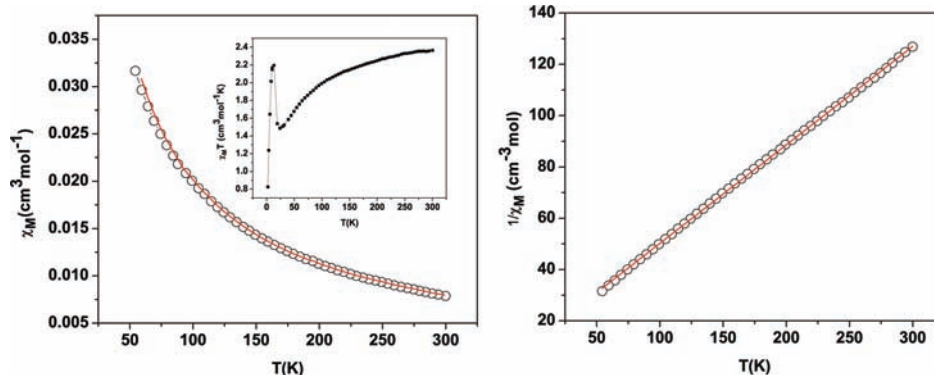


**Figure 4.** Plots of  $\chi_M$  versus  $T$  and  $\chi_M T$  versus  $T$  (inset) (left) where the red lines indicate theoretical fittings; fitting of  $\chi_M^{-1}$  versus  $T$  data using the Curie–Weiss equation in the range 50–300 K (right).

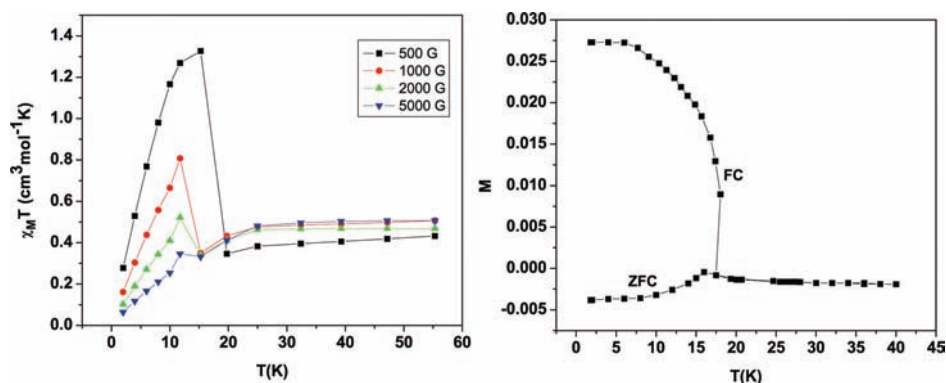


**Figure 5.** Field dependent  $\chi_M T$  in the temperature range of 2–60 K (left); and FC/ZFC magnetizations versus  $T$  plots at 10 G for complex **1** (right).

indicates the presence of dominant antiferromagnetic interaction between two Co(II) paramagnetic centers. Further cooling results in a sudden increase in  $\chi_M T$  to  $2.19 \text{ cm}^3 \text{ mol}^{-1} \text{ K}$  at 13 K before further fall to a minimum value of  $0.82 \text{ cm}^3 \text{ mol}^{-1} \text{ K}$  at 2 K, which could be due to intermolecular antiferromagnetic interaction or spin canting followed by the effect of saturation phenomena. The dominant antiferromagnetic coupling mainly mediates through the  $\mu_{1,3}\text{-N}_3^-$  pathway between two Co(II) centers in complex **1** at high temperature. This was justified by the negative coupling constant  $J = -3.8 \text{ cm}^{-1}$ ,  $\lambda = -5.4 \text{ K}$  obtained upon fitting  $\chi_M$  versus  $T$  above 50 K (Figure 4) using spin-only dimeric model incorporating  $\lambda$  as a correction term which takes care of both interdimer interaction as well as the orbital contribution due to the presence of spin–orbit coupling in the Co(II) system (Supporting Information).<sup>33</sup> Moreover,  $\chi_M^{-1}$  versus  $T$  data above 50 K obey the Curie–Weiss law with the best-fitting parameters  $C = 3.2 \text{ cm}^3 \text{ mol}^{-1} \text{ K}$  [close to the value of  $2.8\text{--}3.4 \text{ cm}^3 \text{ mol}^{-1} \text{ K}$  expected for an octahedral Co(II) ion] and Weiss constant  $\theta = -27.05 \text{ K}$  (Figure 4). The negative  $\theta$  (Weiss constant) value also indicates the existence of antiferromagnetic interaction at high temperature. However, an abrupt rise in  $\chi_M T$  value below 23 K suggests a ferromagnetic transition in complex **1**. Since the saturation value of magnetization [ $0.5 \text{ N}\beta$  per Co(II) at 4 T] is well below the expected value ( $M_s = 2.1\text{--}2.5 \text{ N}\beta$ ), the observed ferromagnetic like

ordering is attributed to canted antiferromagnetism where perfect antiparallel alignment of the spins on neighboring metal ions in **1** is not achieved and leads to the generation of residual spins.

Below 20 K, the susceptibility data become field dependent (Figure 5), suggesting a ferromagnetic phase transition at around 15 K. For further proof of the presence of long-range ordering, zero-field-cooled (ZFC) and field-cooled (FC) magnetization experiments were (Figure 5) carried out at an applied field of 10 G. The ZFC curve increases as the temperature rises from 2 K and reaches a maximum at 15.9 K followed by gradual fall upon further increasing temperature, which is the signature of magnetic ordering. Upon cooling, the FC curve increase rapidly and diverges from the ZFC curve at 15.9 K because of the existence of spontaneous ferromagnetic ordering at  $T_c$  (Curie temperature) = 15.9 K.

At 2 K, complex **1** shows a magnetic hysteresis loop (Figure 6) with a coercive field of 1351.11 G and a remnant magnetization of  $0.05 \text{ N}\beta$ . The estimated canting angle was found to be  $0.95^\circ$  obtained from the equation  $\psi = \sin^{-1}(M_r/M_s)$ ,<sup>34</sup> where  $M_r$  is remnant magnetization

(33) Cheng, X.-N.; Zhang, W.-X.; Chen, X.-M. *J. Am. Chem. Soc.* **2007**, *129*, 15738.

(34) (a) Cave, D.; Gascon, J.-M.; Bond, A. D.; Teat, S. J.; Wood, P. T. *Chem. Commun.* **2002**, 1050. (b) Yoon, J. H.; Lim, J. H.; Choi, S. W.; Kim, H. C.; Hong, C. S. *Inorg. Chem.* **2007**, *46*, 1529. (c) Gao, E.-Q.; Wang, Z.-M.; Yan, C.-H. *Chem. Commun.* **2003**, 1748. (d) Huang, Y.-G.; Yuan, D.-Q.; Pan, L.; Jiang, F.-L.; Wu, M.-Y.; Zhang, X.-D.; Wei, W.; Gao, Q.; Lee, J. Y.; Li, J.; Hong, M.-C. *Inorg. Chem.* **2007**, *46*, 9609. (e) Palacio, F.; Andres, M.; Horne, R.; van Duynveldt, A. J. *J. Magn. Magn. Mater.* **1986**, *54–57*, 1487. (f) Marvilliers, A.; Parsons, S.; Riviere, E.; Audiere, J.-P.; Kurmoo, M.; Mallah, T. *Eur. J. Inorg. Chem.* **2001**, 1287.

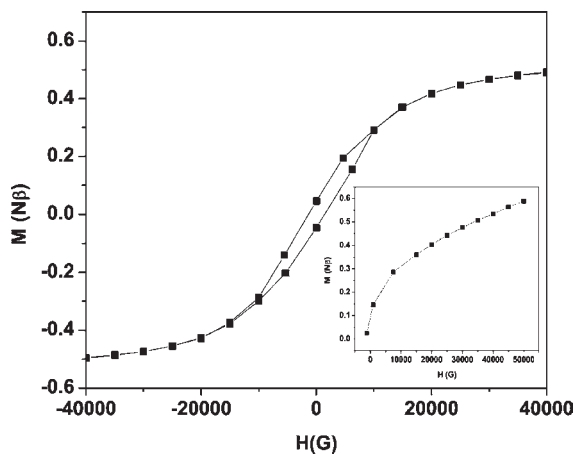


**Figure 6.** Hysteresis plot of complex **1** at 2 K in the field range of  $-4$  to  $+4$  T with initial magnetization plot at 2 K up to 5 T (inset).

and  $M_s$  ( $M_s = gS$ ) is the expected saturated magnetization if all the moments are aligned ferromagnetically. The initial magnetization plot at 2 K shows gradual increase in magnetization with the field. Up to 5 T no saturation in magnetization was noticed, rather magnetization increases linearly with field in the high field region. The magnetization value at 5 T is measured to be  $0.6 N\beta$ , which is far below the expected value for a Co(II) system with  $S = 3/2$  when all the spins are aligned parallel. This nature is consistent with weak ferromagnetism because of presence of spin canted phenomena in complex **1** (Figure 6).

Existence of dominant antiferromagnetic behavior is indicated by the negative  $\theta$  value obtained from the fitting of  $\chi_M^{-1}$  versus  $T$  plot using the Curie–Weiss equation. Moreover, this behavior is expected because of having end-to-end azido antiferromagnetic pathway between the Co(II) centers. However, at lower temperature because of deviation of spins from their normal antiparallel alignment results in a hysteresis loop at 2 K and causes an abrupt rise in magnetization below 23 K. This result suggests a weak ferromagnetic transition at the low temperature region because of spin canting for which complex **1** behaves like a soft magnet.

**Magnetic Study of 2.** The dc magnetic susceptibility data were measured on a crystalline sample of **2** under an applied field of 500 G in the temperature range of 2–300 K using SQUID magnetometer. The  $\chi_M T$  value per Mn(II) center was found to be  $3.08 \text{ cm}^3 \text{ mol}^{-1} \text{ K}$  at 300 K (Figure 7) which is lower than the spin only value ( $4.34 \text{ cm}^3 \text{ mol}^{-1} \text{ K}$ ) expected for a magnetically isolated high spin Mn(II) ion, indicated the occurrence of antiferromagnetic coupling between the Mn(II) centers. Upon cooling,  $\chi_M T$  value gradually decreases to  $2.95 \text{ cm}^3 \text{ mol}^{-1} \text{ K}$  at 53.5 K before it reaches a maximum value of  $4.04 \text{ cm}^3 \text{ mol}^{-1} \text{ K}$  at 34 K. This sharp rise in magnetization is an indication of some sort of ferromagnetic interaction below 40 K. Finally a sudden fall in the magnetization value to  $2.52 \text{ cm}^3 \text{ mol}^{-1} \text{ K}$  at 2 K was noticed which could be due to intermolecular antiferromagnetic interaction. The magnetization data above 60 K obeys the Curie–Weiss law with  $C = 4.4 \text{ cm}^3 \text{ mol}^{-1} \text{ K}$  and  $\theta = -7.8 \text{ K}$  (Figure 7) indicating the existence of antiferromagnetic interaction between the neighboring Mn(II)

centers. The 1D chain consists of magnetically uniform paramagnetic Mn(II) centers where two types of magnetic exchange pathways are present. Each Mn(II) dimer is separated alternatively by double end-to-end azide and tetrazole pathways. Though the magnetic coupling via the azide pathway is expected to be dominating, the interaction through the tetrazole bridge cannot be ignored. Hence, the susceptibility data above 60 K were fitted with the theoretical model developed for an  $S = 5/2$  alternating 1D chain with the spin Hamiltonian,  $H = -J_1 \sum S_{2i} S_{2i+1} - J_2 \sum S_{2i+1} S_{2i+2}$  where  $J_1$  and  $J_2$  denote alternate coupling constants (through azide and tetrazole respectively) and  $S$ 's are classical spin operators.<sup>35</sup> This approximation is well-known for Mn(II) ion with  $S = 5/2$ . The best fit parameters thus obtained were  $J_1 = -5.4 \text{ cm}^{-1}$ ,  $J_2 = -0.5 \text{ cm}^{-1}$  for  $g = 2$  with the agreement factor  $R = 1.86 \times 10^{-4}$  (Figure 7). The values of the coupling constants show that up to 60 K the overall magnetic interaction is antiferromagnetic in nature.

However, a ferromagnetic transition was noticed below 50 K from the  $\chi_M T$  versus  $T$  plot. We can interpret this magnetic behavior as a consequence of spin canting that leads to weak ferromagnetism at low temperature. Azide is known to act as a versatile bridging ligand because of its several binding modes that give rise to different magnetic properties. It has been observed that the end-to-end azide bridge ( $\mu_{1,3}\text{-N}_3^-$ ) generally favors antiferromagnetic interaction.<sup>22,23</sup> The analysis of the magnetic data using the alternating chain model of Mn(II) reveals that both the end-to-end azido as well as the tetrazole pathways mediate expected antiferromagnetic interaction. However, magnetic ordering of the uncompensated spins occurs below 50 K. The mechanism behind this may be due to intermolecular interaction via hydrogen bonding (see packing diagram of complex **2** in Supporting Information).<sup>36</sup> Below 40 K three-dimensional magnetic ordering via intermolecular H-bonding occurs.

Isothermal magnetization plot at 2 K (Figure 8) reveals that the magnetization value reaches  $1.18 N\beta$  at 5 T is much less than the expected saturation value of  $5 N\beta$  for one Mn(II) ion with  $S = 5/2$  and  $g = 2$ . Spin canting could be a reason for such low magnetization value. However, no hysteresis loop was observed for complex **2**. The origin of spin canting is either (i) magnetic anisotropy or (ii) antisymmetric exchange where the spins are slightly tilted from their original position.<sup>37</sup> For a non-centrosymmetric space group there is always a probability of structural distortion that can generate magnetic anisotropy at lower temperature. The spin canting effect is more pronounced in the Co(II) system because of its inherent anisotropic nature compared to the isotropic nature of Mn(II) ion. It is the local anisotropy that makes an additional contribution to a large degree of spin canting in Co(II) systems.

(35) (a) Cortés, R.; Drillon, M.; Solans, X.; Lezama, L.; Rojo, T. *Inorg. Chem.* **1997**, *36*, 677. (b) Abu-Youssef, M. A. M.; Drillon, M.; Escuer, A.; Goher, M. A. S.; Mautner, F. A.; Vicente, R. *Inorg. Chem.* **2000**, *39*, 5022. (c) Cano, J.; Journaux, Y.; Goher, M. A. S.; Abu-Youssef, M. A. M.; Mautner, F. A.; Reiß, G. J.; Escuer, A.; Vicente, R. *New J. Chem.* **2005**, *29*, 306.

(36) Rettig, S. J.; Thompson, R. C.; Trotter, J.; Xia, S. *Inorg. Chem.* **1999**, *38*, 1360.

(37) (a) Carlin, R. L. *Magnetochemistry*; Springer-Verlag: Berlin, 1986. (b) Moriya, T. *Phys. Rev.* **1960**, *117*, 635. (c) Armentano, D.; Munno, G. D.; Lloret, F.; Palií, A. V.; Julve, M. *Inorg. Chem.* **2002**, *41*, 2007.



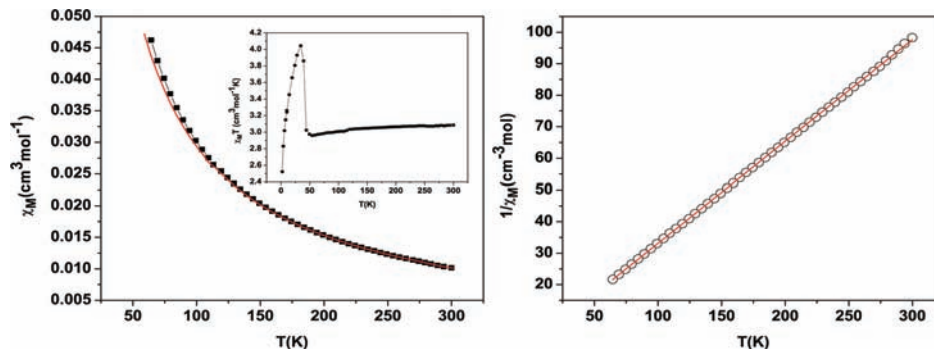


**Figure 7.** Plots of  $\chi_M$  versus  $T$  and  $\chi_M T$  versus  $T$  (inset) (left) where the red lines indicate theoretical fitting (see text); and plot of  $\chi_M^{-1}$  versus  $T$  data fitting using the Curie–Weiss equation in the range 65–300 K (right) for complex **2**.

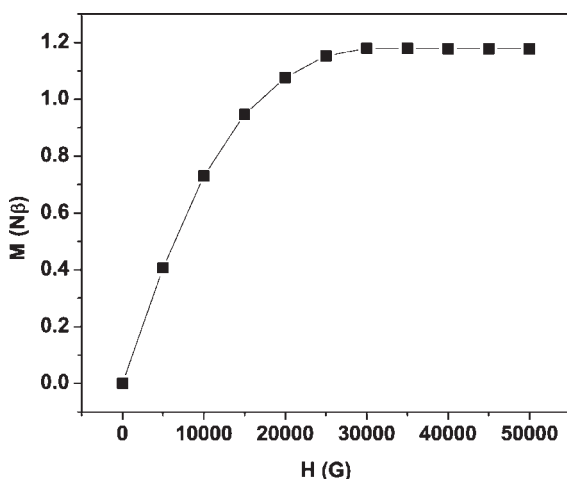


**Figure 8.** Isothermal magnetization plot for complex **2** at 2 K.

**Ferroelectric Study of Complex 1.** Ferroelectric crystals which exhibit a spontaneous electric polarization arising from polar displacements of anions and cations are drawing significant attentions because of their potential applications in the field of telecommunication, ultrasonic devices, electro-optical devices, and switchable NLO (nonlinear optical) devices. Initially ferroelectric behavior was noticed in pure inorganic complexes like KDP, BaTiO<sub>3</sub> but because of various applications of this type of ferroelectric materials, several new kinds of ferroelectric materials have been reported. A literature survey reveals that several metal complexes like Cd(II) imidazole,<sup>38</sup> Ag(I) imidazole,<sup>39</sup> Cu(II) with substituted pyrazole,<sup>40</sup>

Co(II) piperazine complex,<sup>41</sup> and diethyldithiocarbamate complex of Cu(II)<sup>42–44</sup> exhibit ferroelectric behavior. In addition to transition metal complexes, several lanthanides complexes (Sm, Gd, Eu) have also been found to be potentially ferroelectric.<sup>45</sup> A new addition to this ferroelectric material is the template borate of Ni(II) complex.<sup>46</sup> A ferroelectric ferromagnet which is one of the multiferroics has received significant attention because of this multifunctionality. As both ferroelectric and ferromagnetic properties are mutually exclusive, systems with multiferroic behavior are very rare. Among them ethyl lactate complex with Tb, hexacyanoferrate with rubidium, manganese, and dimethylammonium metal formates are some examples which show multiferroic behavior.<sup>26</sup>

Complex **1** in the present study crystallized in a non-centrosymmetric space group *Aba2* which is associated with the point group  $C_{2v}$  that is one of the 10 polar point groups ( $C_1, C_s, C_2, C_{2v}, C_4, C_{4v}, C_3, C_{3v}, C_6, C_{6v}$ ) required for ferroelectric behavior. To our knowledge until now no multiferroic metal-tetrazole complex has been reported. In this respect complex **1** is a novel example which reveals both magnetism and ferroelectricity. The ferroelectric data of the powder pellet sample of **1** were measured at room temperature at different voltages. Polarization ( $P$ ) versus applied electric field ( $E$ ) plots at room temperature with applying field up to  $\pm 30$  KV cm<sup>-1</sup> showed (Figure 9) a clear electric hysteresis loop. The remnant electric polarization ( $P_r$ ) and coercive field ( $E_c$ ) were calculated to be 0.08  $\mu\text{C cm}^{-2}$  and of 4.73 KV cm<sup>-1</sup>, respectively. The saturation spontaneous polarization ( $P_s$ ) of 0.29  $\mu\text{C cm}^{-2}$  is little higher than that of a typical ferroelectric compound NaKC<sub>4</sub>H<sub>4</sub>O<sub>6</sub>·4H<sub>2</sub>O ( $P_s = 0.25 \mu\text{C cm}^{-2}$ ). Interestingly, even at 100 K electric hysteresis loop was clearly noticed at 1500 V with calculated  $P_r$  and  $E_c$  values of 0.09  $\mu\text{C cm}^{-2}$  and 5.14 KV cm<sup>-1</sup>, respectively, having spontaneous polarization  $P_s = 0.28 \mu\text{C cm}^{-2}$  (Figure 9). However, our attempt to establish the ferroelectric behavior below 100 K was unsuccessful because of the limitation of the instrument.

## Conclusion

In summary, two new coordination polymers of transition metals with 5-(pyrimidyl)tetrazole ligand and azide have

(38) (a) Su, Z.; Chen, M.-S.; Fan, J.; Chen, M.; Chen, S.-S.; Luo, L.; Sun, W.-Y. *CrystEngComm* **2010**, *12*, 2040. (b) Wang, Y.-T.; Tang, G.-M.; Wei, Y.-Q.; Qin, T.-X.; Li, T.-D.; He, C.; Ling, J.-B.; Long, X.-F.; Ng, S. W. *Cryst. Growth Des.* **2010**, *10*, 25. (c) Fu, D.-W.; Zhang, W.; Xiong, R.-G. *Dalton Trans.* **2008**, 3946.

(39) Song, L.; Du, S.-W.; Lin, J.-D.; Zhou, H.; Li, T. *Cryst. Growth Des.* **2007**, *7*, 2268.

(40) Xie, Y.-M.; Liu, J.-H.; Wu, X.-Y.; Zhao, Z.-G.; Zhang, Q.-S.; Wang, F.; Chen, S.-C.; Lu, C.-Z. *Cryst. Growth Des.* **2008**, *8*, 3914.

(41) Ye, H.-Y.; Fu, D.-W.; Zhang, Y.; Zhang, W.; Xiong, R.-G.; Huang, S.-D. *J. Am. Chem. Soc.* **2009**, *131*, 42.

(42) Okubo, T.; Kawajiri, R.; Mitani, T.; Shimoda, T. *J. Am. Chem. Soc.* **2005**, *127*, 17598.

(43) Ye, Q.; Song, Y.-M.; Wang, G.-X.; Chen, K.; Fu, D.-W.; Chan, P. W. H.; Zhu, J.-S.; Huang, S. D.; Xiong, R.-G. *J. Am. Chem. Soc.* **2006**, *128*, 6554.

(44) Wen, H.-R.; Tang, Y.-Z.; Liu, C.-M.; Chen, J.-L.; Yu, C.-L. *Inorg. Chem.* **2009**, *48*, 10177.

(45) Li, D.-P.; Wang, T.-W.; Li, C.-H.; Liu, D.-S.; Li, Y.-Z.; You, X.-Z. *Chem. Commun.* **2010**, *46*, 2929.

(46) Pan, C.-Y.; Hu, S.; Li, D.-G.; Ouyang, P.; Zhao, F.-H.; Zheng, Y.-Y. *Dalton Trans.* **2010**, *39*, 5772.

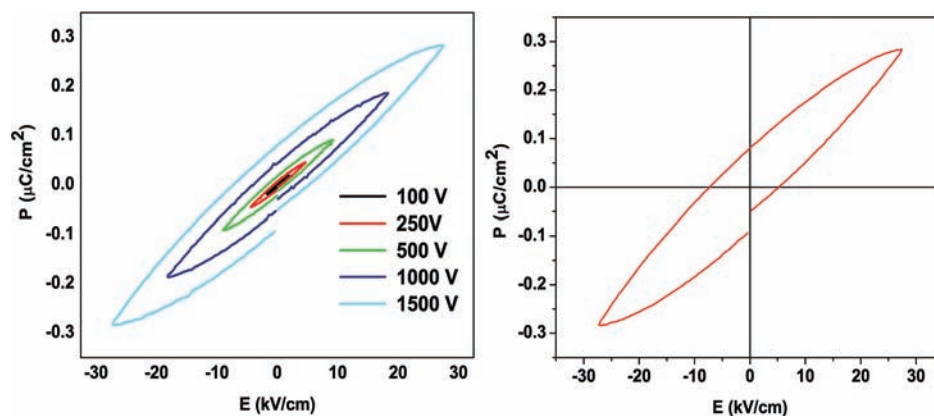


**Figure 9.** Electric hysteresis loop of **1** at different voltages observed for a powdered sample in the form of a pellet using a ferroelectric tester at room temperature (left) and electric hysteresis loop measured at low temperature (right).

been successfully synthesized by the hydrothermal method. Complex **1** crystallized in non-centrosymmetric space group *Aba2* in the orthorhombic system. This complex also showed spin canting behavior with a clear hysteresis loop in the *M* versus *H* plot at low temperature, which is a characteristic of a soft magnet. Complex **1** also showed ferroelectric behavior with electric hysteresis loop at 100 and 300 K. Though several ferroelectric coordination polymers or ferromagnetic coordination polymers are known in the literature, complex **1** represents a rare example which shows both ferroelectric behavior and magnetic hysteresis. Complex **2** crystallized in the *P2<sub>1</sub>/c* space group in the monoclinic system. From structural point of view, complex **2** is a 1D chain of Mn(II) ions bridged by well-known antiferromagnetic coupler end-to-end azido and tetrazolate. Variable temperature magnetic study revealed the existence of an unusual ferromagnetic transition through the end-to-end azido pathway below 40 K as a consequence of spin canting. The present results demonstrate the potential of tetrazole for the generation of

multifunctional materials and further illustrate the versatility of azido as a mediator for magnetic interactions.

**Acknowledgment.** Authors sincerely thank Dr. G. Mostafa of Jadavpur University for his kind help in solving the structure of complex **2**. O.S. gratefully acknowledges Mr. Pranab Mandal and Mr. Yogesh P. Patil for their help on ferroelectric measurements and on structure solution, respectively. P.S.M. thanks the Department of Science and Technology, New Delhi, for financial support. Authors sincerely thank all the referees for their fruitful comments and suggestions.

**Supporting Information Available:** X-ray crystallographic data of **1** and **2** in CIF format, asymmetric unit figures of complex **1** and **2**, selected bond length and bond angle table of complex **1** and **2**, packing diagram of complex **2**, hydrogen bonding table for complex **2** and magnetic data fitting susceptibility equation of complex **1**. This material is available free of charge via the Internet at <http://pubs.acs.org>.